Two-dimensional relativistic longitudinal Green's function in the presence of a moving planar dielectric–magnetic discontinuity

Tatiana Danov and Timor Melamed*

Department of Electrical and Computer Engineering, Ben-Gurion University of the Negev, Beer Sheva 84105, Israel
**Corresponding author: timormel@ee.bgu.ac.il*

Received September 19, 2011; revised October 23, 2011; accepted October 26, 2011;
posted October 26, 2011 (Doc. ID 154988); published February 14, 2012

The current contribution is concerned with obtaining the relativistic two-dimensional (three-dimensional in relativity jargon) Green's function of a time-harmonic line current that is embedded in a moving dielectric–magnetic medium with a planar discontinuity. By applying a plane-wave (PW) spectral representation for the relativistic electromagnetic Green's function of a dielectric–magnetic medium that is moving in a uniform velocity, the exact reflected and transmitted (refracted) fields are obtained in the form of a spectral integral over PWs in the so-called laboratory and comoving frames. We investigate these spectral representations, as well as their asymptotic evaluations, and discuss the associated relativistic wave phenomena of direct reflected/transmitted rays and relativistic head waves (lateral waves).

OCIS codes: 350.5720, 080.0080, 290.5825, 050.1960.

1. INTRODUCTION AND STATEMENT OF THE PROBLEM

Green's functions of electromagnetic (EM) wave propagation in a moving medium have been a subject of a continuing research [1–4]. The dyadic Green's functions of an homogeneous isotropic dielectric–magnetic medium have been derived in closed form in [5] and an alternative simple derivation was presented in [6].

Plane-wave (PW) spectral representations have been an important tool for solving relativistic scattering and diffraction problems. Such spectral representations have been utilized for scattering of a PW by a uniformly moving perfectly conducting half-plane [7], for the two-dimensional problem of the uniformly moving perfectly conducting cylinder [8], for solving the EM field radiated by an infinitely long thin wire antenna that uniformly translates in a direction parallel to a plane interface [9], for the EM radiation from fractal antennas [10], and for EM wave scattering from moving rough surfaces [11].

EM scattering from moving objects is of fundamental importance in antenna and scattering theory, cellular and satellite communication, radar applications, inverse scattering, remote sensing, and more. Although impressive advances have been made in this field, little effort has been made to adjust basic stationary wave theories [such as the geometrical theory of diffraction (GTD), the uniform theory of diffraction, and direct time-domain methods] to the scatterer dynamics. Basic wave phenomena of relativistic scattering, such as high-frequency/short-pulsed canonical forms and diffraction coefficients, are not yet fully understood. Furthermore, little attention has been given to problems concerning scattering in a moving dielectric medium where the electrodynamics introduces wave phenomena that are unique to special relativity and that are not found in classical (stationary) GTD, such as relativistic lateral waves and their wave phenomena, Čerenkov-type scattering and its high-frequency forms, and more.

Recently, a PW spectral representation of the relativistic electric and magnetic dyadic Green's functions of a uniformly moving dielectric–magnetic medium was obtained in [12]. By applying a simple coordinate transformation, scalarization of the EM vectorial problem was obtained in which the EM dyads are evaluated from Helmholtz's free-space (isotropic) scalar Green's function. The spectral PW representations of the dyadic Green's functions were obtained by applying the spatial two-dimensional (2D) Fourier transform to the scalar Green's function in both the under and over phase-speed medium velocity regimes.

In the current work, we apply the spectral representations in [12] in order to obtain the EM Green's function of a time-harmonic line current that is located at $(y,z)=(0,0)$ and is embedded in a uniformly moving dielectric–magnetic medium with a planar discontinuity. In K-frame, the medium is moving in a constant translation velocity $\mathbf{v}=v\hat{\mathbf{z}}$, where we assume that the velocity is in the direction of the z axis. Unit vectors in the conventional Cartesian coordinate system, (x,y,z), are denoted by a hat over bold fonts. Under the framework of special relativity, a three-dimensional (space–time) event (y,z,t) in the so-called laboratory frame (K-frame) is mapped to the event (y',z',t') in the comoving frame (K'-frame) by the Lorentz transformation (LT) and the inverse LT (ILT), which are defined for the K'-frame velocity of $\mathbf{v}=v\hat{\mathbf{z}}$ by

$$y'=y,\qquad z'=\gamma(z-\beta ct),\qquad t'=\gamma(t-\beta z/c),\tag{1}$$

$$y=y',\qquad z=\gamma(z'+\beta ct'),\qquad t=\gamma(t'+\beta z'/c),\tag{2}$$

where $c=1/\sqrt{\epsilon_0\mu_0}$ is the speed of light in vacuum and

$$\beta = v/c, \qquad \gamma = 1/\sqrt{1-\beta^2}. \tag{3}$$

Here and henceforth, all physical quantities in the K'-frame are denoted by a prime. The EM field transformation that is corresponding to $\mathbf{v} = v\hat{\mathbf{z}}$ is given by [13]

$$\begin{aligned} \mathbf{E}'(\mathbf{r}', t') &= \underline{\mathbf{V}} \cdot [\mathbf{E} + \mathbf{v} \times \mathbf{B}], \\ \mathbf{B}'(\mathbf{r}', t') &= \underline{\mathbf{V}} \cdot [\mathbf{B} - \mathbf{v} \times \mathbf{E}/c^2], \\ \mathbf{D}'(\mathbf{r}', t') &= \underline{\mathbf{V}} \cdot [\mathbf{D} + \mathbf{v} \times \mathbf{H}/c^2], \\ \mathbf{H}'(\mathbf{r}', t') &= \underline{\mathbf{V}} \cdot [\mathbf{H} - \mathbf{v} \times \mathbf{D}], \end{aligned} \tag{4}$$

where $\mathbf{r}' = (y', z')$, the $\mathbf{r} = (y, z)$ and t coordinates are transformed into $(\mathbf{r}', t')$ via ILT in Eq. (2), and the (diagonal) dyadic $\underline{\mathbf{V}}$ is given by

$$\underline{\mathbf{V}} = \mathrm{diag}\{\gamma, \gamma, 1\}. \tag{5}$$

Here and henceforth, underlined boldfaced letters denote matrices/dyads. The inverse of Eq. (4) is form invariant and thus can be obtained by interchanging all primed and unprimed quantities where $\underline{\mathbf{V}}' = \underline{\mathbf{V}}$ and $\mathbf{v}' = -\mathbf{v}$.

We are aiming at obtaining the relativistic 2D (3D in relativity jargon) Green's function of the time-harmonic line current,

$$\mathbf{J}(\mathbf{r}, t) = I_0 \delta(z)\delta(y)\exp(j\omega t)\hat{\mathbf{x}}, \tag{6}$$

that is located in the so-called laboratory K-frame at $\mathbf{r} = (y, z) = (0, 0)$ (see Fig. 1). The source is embedded in a uniformly moving dielectric–magnetic medium with a planar discontinuity. The medium's discontinuity is located at $z = z_0 > 0$ at time $t = 0$ in K-frame. The medium is assumed to be a linear isotropic dielectric–magnetic in the frame at rest (the "comoving" K'-frame) with $\epsilon'_{1,2}$ and $\mu'_{1,2}$ denoting its permittivity and permeability, where indices 1 and 2 refer to either side of the discontinuity. Thus, the constitutive relations in K'-frame are

$$\begin{aligned} \mathbf{D}' &= \epsilon'_1 \mathbf{E}', \qquad \mathbf{B}' = \mu'_1 \mathbf{H}', \qquad z' < z'_0, \\ \mathbf{D}' &= \epsilon'_2 \mathbf{E}', \qquad \mathbf{B}' = \mu'_2 \mathbf{H}', \qquad z' > z'_0, \end{aligned} \tag{7}$$

where $z'_0 = \gamma z_0$ denotes the interface location in K'-frame, which is obtained from LT in Eq. (1). In the current contribution, we assume that the medium is lossless and dispersion free and that its velocity does not exceed the K'-frame phase velocities of $c/\sqrt{\epsilon'_{1,2}\mu'_{1,2}}$.

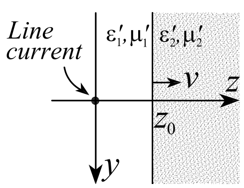

Fig. 1. Physical configuration of the relativistic Green's function of a line current that is embedded in a dielectric–magnetic medium with a planar discontinuity. The medium is uniformly moving in the z direction with a velocity of $\mathbf{v} = v\hat{\mathbf{z}}$ in the laboratory frame and the discontinuity is located in $z = z_0$ at $t = 0$. The medium is an isotropic dielectric–magnetic in the comoving frame with $\varepsilon'_{1,2}$ and $\mu'_{1,2}$ denoting its permittivity and permeability on either side of the discontinuity.

The outline of the paper is as follows: in Section 2 we briefly describe the spectral representation of the incident field that was derived in [12] and, in Section 3, the spectral representation of the Green's function in the presence of a moving discontinuity is obtained by applying Maxwell's boundary conditions in K'-frame. The spectral representation is obtained in both K'- and K-frames of reference in Subsections 3.A and 3.B, respectively. The *asymptotic* evaluations of the incident, reflected, and transmitted (refracted) waves in the high-frequency regime are obtained in Sections 4 and 5 for fields in K'- and K-frames, respectively.

2. SPECTRAL REPRESENTATION OF THE INCIDENT FIELD

The incident EM field in K-frame is the field that is radiated by the current line source in Eq. (6). The line current is embedded in a uniformly moving dielectric–magnetic medium of (K') permittivity and permeability of ε'_1 and μ'_1, respectively (for all $\mathbf{r}'$). In K-frame, the corresponding constitutive relations can be stated as [6]

$$\begin{aligned} \mathbf{D} &= \epsilon'_1 \underline{\boldsymbol{\alpha}} \cdot \mathbf{E} + c^{-1} m \hat{\mathbf{z}} \times \mathbf{H}, \\ \mathbf{B} &= \mu'_1 \underline{\boldsymbol{\alpha}} \cdot \mathbf{H} - c^{-1} m \hat{\mathbf{z}} \times \mathbf{E}, \end{aligned} \tag{8}$$

where

$$m = \beta \frac{n_1'^2 - 1}{1 - n_1'^2 \beta^2}, \qquad n'_1 = c\sqrt{\epsilon'_1 \mu'_1}, \tag{9}$$

and $\underline{\boldsymbol{\alpha}}$ is the diagonal matrix

$$\underline{\boldsymbol{\alpha}} = \mathrm{diag}\{\alpha, \alpha, 1\}, \qquad \alpha = \frac{1 - \beta^2}{1 - n_1'^2 \beta^2}. \tag{10}$$

The spectral representation of the incident EM field that is denoted by $\mathbf{E}^i(\mathbf{r}, t)$ can be obtained by formulating the current source Green's function in K'-frame where the constitutive relations have simple expressions, while the source density function involves distributions that are moving along the z axis with velocity v (see, for example, [14]). In the current contribution we use the results that were obtained in [12] in which the incident EM field was derived directly in K-frame by using the normalized longitudinal coordinate and wavenumber

$$\bar{z} = \sqrt{\alpha} z, \qquad \bar{k}_1 = \omega\sqrt{\alpha \epsilon'_1 \mu'_1}. \tag{11}$$

Note that m in Eq. (9) and α in Eq. (10) are positive (assuming that the medium velocity does not exceed the medium's phase velocity of c/n'_1) so that $\sqrt{\alpha} > 0$ is real.

By using these definitions, the incident electric field is decomposed into PWs in the form

$$\mathbf{E}^i(\mathbf{r}, t) = \frac{1}{2\pi} \int \mathrm{d}k_y \tilde{\mathbf{E}}^i(\mathbf{r}, t; k_y), \tag{12}$$

where the incident electric field spectral PWs that are denoted by $\tilde{\mathbf{E}}^i$ are given by

$$\begin{aligned} \tilde{\mathbf{E}}^i(\mathbf{r}, t; k_y) &= -\frac{I_0 \omega \mu'_1 \sqrt{\alpha}}{2\bar{k}_{z_1}} \hat{\mathbf{x}} \exp(j\Psi^i), \\ \Psi^i &= \omega t - k_y y - \bar{k}_{z_1} \bar{z} + kmz, \end{aligned} \tag{13}$$

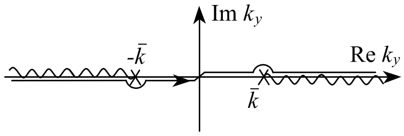

Fig. 2. Integration contour of the PW spectral representation in Eq. (14). The upper Riemann sheet is define by $\mathrm{Re}\,\bar{k}_{z_1} \geq 0$.

where $k = \omega/c$ is the wavenumber in vacuum, and the longitudinal wavenumber that is denoted by $\bar{k}_{z_1}$ is given by

$$\bar{k}_{z_1} = \sqrt{\bar{k}_1^2 - k_y^2}, \qquad \mathrm{Re}\,\bar{k}_{z_1} \geq 0, \qquad \mathrm{Im}\,\bar{k}_{z_1} \leq 0. \tag{14}$$

Here and henceforth, over tilde ($\sim$) denotes PW constituents. The integration contour is described in Fig. 2 where the upper Riemann sheet is define by $\mathrm{Re}\,\bar{k}_{z_1} \geq 0$.

The integral in Eq. (12) represents the incident electric field as a superposition of the spectral PWs in $z > 0$ half-space. Propagating PWs occur for spectral wavenumbers $|k_y| \leq \bar{k}_1$. For all other k_y values, $\bar{k}_{z_1}$ is imaginary and the PWs are evanescent and decay exponentially away from the source location. The incident magnetic field that is denoted by $\mathbf{H}^i(\mathbf{r}, t)$ is given by the PW spectral integral

$$\mathbf{H}^i(\mathbf{r}, t) = \frac{1}{2\pi}\int \mathrm{d}k_y \tilde{\mathbf{H}}^i(\mathbf{r}, t; k_y), \tag{15}$$

over the magnetic spectral PWs

$$\tilde{\mathbf{H}}^i(\mathbf{r}, t; k_y) = \frac{I_0}{2\bar{k}_{z_1}}(-\bar{k}_{z_1}\hat{\mathbf{y}} + \sqrt{\alpha}k_y\hat{\mathbf{z}})\exp(j\Psi^i), \tag{16}$$

where Ψ^i is given in (13).

The scattering wave is obtained by transforming the incident EM field spectral PWs in Eqs. (13) and (16) to the K'-frame and applying Maxwell's boundary conditions at the interface. By inserting Eqs. (12) and (15) into Eq. (8), we obtain the electric displacement and magnetic flux density spectral PW representations, which are required for the EM field transformation in (4). Thus

$$\mathbf{D}^i(\mathbf{r}, t) = \frac{1}{2\pi}\int \mathrm{d}k_y \tilde{\mathbf{D}}^i(\mathbf{r}, t; k_y),$$
$$\mathbf{B}^i(\mathbf{r}, t) = \frac{1}{2\pi}\int \mathrm{d}k_y \tilde{\mathbf{B}}^i(\mathbf{r}, t; k_y), \tag{17}$$

where the corresponding spectral PWs fields are

$$\tilde{\mathbf{D}}^i(\mathbf{r}, t; k_y) = -\frac{I_0}{2\bar{k}_{z_1}}\left(\omega\mu_1'\varepsilon_1'\alpha^{3/2} - \frac{m\bar{k}_{z_1}}{c}\right)\hat{\mathbf{x}}\exp(j\Psi^i),$$
$$\tilde{\mathbf{B}}^i(\mathbf{r}, t; k_y) = -\frac{\mu_1'\sqrt{\alpha}I_0}{2\bar{k}_{z_1}}\left[\left(\sqrt{\alpha}\bar{k}_{z_1} - \frac{m\omega}{c}\right)\hat{\mathbf{y}} - k_y\hat{\mathbf{z}}\right]\exp(j\Psi^i). \tag{18}$$

3. SPECTRAL REPRESENTATION OF GREEN'S FUNCTION

In this section we derive the spectral representations of the reflected and transmitted waves on either side of the interface, $z' \lessgtr z_0'$.

A. Fields in K'-Frame

By inserting the spectral representations in Eqs. (12), (15), and (17) into the field transformation in Eq. (4) and using the LT in Eq. (1), we obtain the spectral integral of the incident EM field in K'-frame:

$$\mathbf{E}^{i'}(\mathbf{r}', t') = \frac{1}{2\pi}\int \mathrm{d}k_y \tilde{\mathbf{E}}^{i'}(\mathbf{r}', t'; k_y),$$
$$\mathbf{H}^{i'}(\mathbf{r}', t') = \frac{1}{2\pi}\int \mathrm{d}k_y \tilde{\mathbf{H}}^{i'}(\mathbf{r}', t'; k_y), \tag{19}$$

where the spectral PWs are given by

$$\tilde{\mathbf{E}}^{i'}(\mathbf{r}', t'; k_y) = -\tilde{E}_0'\hat{\mathbf{x}}\exp(j\Psi^{i'}),$$
$$\tilde{\mathbf{H}}^{i'}(\mathbf{r}', t'; k_y) = -\frac{1}{\eta_1'}\frac{\omega}{\omega'}\tilde{E}_0'\left[\gamma\alpha\left(\frac{\bar{k}_{z_1}}{\bar{k}_1} - n_1'\beta\right)\hat{\mathbf{y}} - \frac{k_y\sqrt{\alpha}}{\bar{k}_1}\hat{\mathbf{z}}\right]$$
$$\times\exp(j\Psi^{i'}). \tag{20}$$

Here $\eta_1' = \sqrt{\mu_1'/\varepsilon_1'}$, n_1' is given in Eq. (9), $\bar{k}_{z_1}$ is given by Eq. (14), the amplitude $\tilde{E}_0'$ is given by

$$\tilde{E}_0' = \frac{I_0\omega\mu_1'\alpha^{3/2}}{2\bar{k}_{z_1}}\gamma(1 - n_1'\beta\bar{k}_{z_1}/\bar{k}_1), \tag{21}$$

and the phase $\Psi^{i'}$ is given by

$$\Psi^{i'}(\mathbf{r}', t'; k_y) = \omega't' - k_y y' - k_{z_1}' z', \tag{22}$$

where

$$\omega' = \omega\gamma\alpha(1 - n_1'\beta\bar{k}_{z_1}/\bar{k}_1), \qquad k_{z_1}' = \sqrt{\alpha}\gamma(\bar{k}_{z_1} - n_1'\beta\bar{k}_1) \tag{23}$$

are identified as the temporal frequency (Doppler shift) and the longitudinal wavenumber of the spectral PW in K'-frame.

Next we define normalized z' and t' coordinates:

$$\bar{z}' = \sqrt{\alpha}\gamma z', \qquad \bar{t}' = \sqrt{\alpha}\gamma t', \tag{24}$$

and recast Eq. (22) in the form

$$\Psi^{i'}(\mathbf{r}', t'; k_y) = \bar{\omega}'\bar{t}' - k_y y' - \bar{k}_{z_1}'\bar{z}', \tag{25}$$

where we define the *normalized* frequency and longitudinal wavenumber:

$$\bar{\omega}' \equiv \omega'/\sqrt{\alpha}\gamma = \omega\sqrt{\alpha}(1 - n_1'\beta\bar{k}_{z_1}/\bar{k}_1),$$
$$\bar{k}_{z_1}' \equiv k_{z_1}'\sqrt{\alpha}\gamma = (\bar{k}_{z_1} - n_1'\beta\bar{k}_1). \tag{26}$$

The reflected and transmitted fields on either side of the (stationary) interface at $z' = z_0'$ can be obtained from the well-known results of PW scattering from stationary dielectric–magnetic planar discontinuity (i.e., the Fresnel coefficients) since, for a given k_y, the incident spectral PW is a time-harmonic field that carries the temporal frequency of ω' in Eq. (23). Thus, the reflected EM field, which is denoted by $\mathbf{E}^{r'}$ and $\mathbf{H}^{r'}$, is given by a spectral representation similar to Eqs. (12) and (15):

$$\mathbf{E}^{r'}(\mathbf{r}',t') = \frac{1}{2\pi}\int \mathrm{d}k_y \tilde{\mathbf{E}}^{r'}(\mathbf{r}',t';k_y),$$
$$\mathbf{H}^{r'}(\mathbf{r}',t') = \frac{1}{2\pi}\int \mathrm{d}k_y \tilde{\mathbf{H}}^{r'}(\mathbf{r}',t';k_y), \tag{27}$$

over their spectral PWs

$$\tilde{\mathbf{E}}^{r'}(\mathbf{r}',t';k_y) = -\tilde{E}_0'\Gamma'(k_y)\hat{\mathbf{x}}\exp(j\Psi^{r'}),$$
$$\tilde{\mathbf{H}}^{r'}(\mathbf{r}',t';k_y) = \frac{1}{\eta_1'}\Gamma'(k_y)\tilde{E}_0'\frac{\gamma^{-1}}{\bar{k}_1}\frac{\omega}{\bar{\omega}'}(k_{z_1}'\hat{\mathbf{y}} + k_y\hat{\mathbf{z}})\exp(j\Psi^{r'}). \tag{28}$$

Here ω' is given in Eq. (23) and the phase $\Psi^{r'}$ is given by

$$\Psi^{r'}(\mathbf{r}',t';k_y) = \bar{\omega}'\bar{t}' - k_y y' - \bar{k}_{z_1}'(2\bar{z}_0' - \bar{z}'), \tag{29}$$

with $\bar{z}'$ in Eq. (24) and $\bar{z}_0' = \sqrt{\alpha}\gamma z_0'$. In Eq. (28), $\Gamma'(k_y)$ denotes the Fresnel reflection coefficient [13]:

$$\Gamma'(k_y) = \frac{\mu_2'\bar{k}_{z_1}' - \mu_1'\bar{k}_{z_2}'}{\mu_2'\bar{k}_{z_1}' + \mu_1'\bar{k}_{z_2}'}, \tag{30}$$

where

$$\bar{k}_{z_2}' = \sqrt{\bar{\omega}'^2\varepsilon_2'\mu_2' - k_y^2/\alpha\gamma^2}, \tag{31}$$

and $\bar{\omega}'$ and $\bar{k}_{z_1}'$ are given in Eq. (26).

Similarly, the *transmitted* field that is propagating in $z' > z_0'$ is given by the spectral integrations

$$\mathbf{E}^{t'}(\mathbf{r}',t') = \frac{1}{2\pi}\int \mathrm{d}k_y \tilde{\mathbf{E}}^{t'}(\mathbf{r}',t';k_y),$$
$$\mathbf{H}^{t'}(\mathbf{r}',t') = \frac{1}{2\pi}\int \mathrm{d}k_y \tilde{\mathbf{H}}^{t'}(\mathbf{r}',t';k_y), \tag{32}$$

over the transmitted spectral PWs

$$\tilde{\mathbf{E}}^{t'}(\mathbf{r}',t';k_y) = -\tilde{E}_0'T'(k_y)\hat{\mathbf{x}}\exp(j\Psi^{t'}),$$
$$\tilde{\mathbf{H}}^{t'}(\mathbf{r}',t';k_y) = -\frac{1}{\omega'\mu_2'}\tilde{E}_0'T'(k_y)(k_{z_2}'\hat{\mathbf{y}} - k_y\hat{\mathbf{z}})\exp(j\Psi^{t'}), \tag{33}$$

where the phase $\Psi^{t'}$ is given by

$$\Psi^{t'}(\mathbf{r}',t';k_y) = \bar{\omega}'\bar{t}' - k_y y' - \bar{k}_{z_2}'(\bar{z}' - \bar{z}_0') - \bar{k}_{z_1}'\bar{z}_0', \tag{34}$$

and the transmission coefficient $T'(k_y)$ of the interface at $z' = z_0'$ is given by

$$T'(k_y) = 1 + \Gamma'(k_y). \tag{35}$$

The spectral PWs in Eq. (33) are propagating in $(y', z' > z_0')$ half-space in the direction of the unit vector $\hat{\kappa}^{t'} = \hat{\mathbf{y}}\sin\varphi^{t'} + \hat{\mathbf{z}}\cos\varphi^{t'}$ where, by using the phase $\Psi^{t'}$ in Eqs. (34) and (31), we obtain

$$\sin\varphi^{t'} = \frac{k_y}{\bar{\omega}'\sqrt{\alpha}\gamma\sqrt{\varepsilon_2'\mu_2'}}. \tag{36}$$

B. Fields in *K*-Frame

The spectral integral of the reflected EM fields in K-frame are obtained by inserting Eqs. (27) and (28) with Eq. (7) into Eq. (4) and using the ILT in Eq. (2). The resulting spectral integrals of the EM fields are

$$\mathbf{E}^{r}(\mathbf{r},t) = \frac{1}{2\pi}\int \mathrm{d}k_y \tilde{\mathbf{E}}^{r}(\mathbf{r},t;k_y),$$
$$\mathbf{H}^{r}(\mathbf{r},t) = \frac{1}{2\pi}\int \mathrm{d}k_y \tilde{\mathbf{H}}^{r}(\mathbf{r},t;k_y), \tag{37}$$

over the spectral PWs

$$\tilde{\mathbf{E}}^{r}(\mathbf{r},t;k_y) = -\hat{\mathbf{x}}\tilde{E}_0'\Gamma'(k_y)\left(1 - n_1'\beta\sqrt{\alpha}\frac{\omega\bar{k}_{z_1}'}{\bar{\omega}'\bar{k}_1}\right)\gamma\exp(j\Psi^{r}),$$
$$\tilde{\mathbf{H}}^{r}(\mathbf{r},t;k_y) = \frac{\tilde{E}_0'\Gamma'(k_y)}{\eta_1'}\left(\gamma\frac{\omega\sqrt{\alpha}\bar{k}_{z_1}' - \bar{\omega}'n_1'\beta\bar{k}_1}{\bar{\omega}'\bar{k}_1 - \omega n_1'\beta\sqrt{\alpha}\bar{k}_{z_1}}\hat{\mathbf{y}} + \frac{\omega}{\bar{\omega}'}\frac{k_y\gamma^{-1}}{\bar{k}_1}\hat{\mathbf{z}}\right)$$
$$\times\exp(j\Psi^{r}). \tag{38}$$

Here $\bar{\omega}'$ is given in Eq. (26) and the phase Ψ^{r} is given by

$$\Psi^{r}(\mathbf{r},t;k_y) = \sqrt{\alpha}\gamma^2(\bar{\omega}' - \beta c\bar{k}_{z_1}')t - k_y y$$
$$- \sqrt{\alpha}\gamma^2[\bar{\omega}'\beta c^{-1}z + \bar{k}_{z_1}'(2z_0 - z)]. \tag{39}$$

The spectral integrals in Eq. (37) are evaluated asymptotically in Section 5.

The spectral integrals of the *transmitted* EM field in K-frame are obtained by inserting Eqs. (32) and (33) with Eq. (7) into Eq. (4) and using ILT in Eq. (2). This procedure yields

$$\mathbf{E}^{t}(\mathbf{r},t) = \frac{1}{2\pi}\int \mathrm{d}k_y \tilde{\mathbf{E}}^{t}(\mathbf{r},t;k_y),$$
$$\mathbf{H}^{t}(\mathbf{r},t) = \frac{1}{2\pi}\int \mathrm{d}k_y \tilde{\mathbf{H}}^{t}(\mathbf{r},t;k_y), \tag{40}$$

where the spectral PWs are given by

$$\tilde{\mathbf{E}}^{t}(\mathbf{r},t;k_y) = -\tilde{E}_0'T'(k_y)\gamma\left(1 + c\beta\frac{\bar{k}_{z_2}'}{\bar{\omega}'}\right)\hat{\mathbf{x}}\exp(j\Psi^{t}),$$
$$\tilde{\mathbf{H}}^{t}(\mathbf{r},t;k_y) = -\frac{1}{\eta_2'}\tilde{E}_0'T'(k_y)\left[\gamma\left(n_2'\beta + \frac{c\bar{k}_{z_2}'}{n_2'\bar{\omega}'}\right)\hat{\mathbf{y}} - \frac{ck_y}{n_2'\bar{\omega}'}\hat{\mathbf{z}}\right]$$
$$\times\exp(j\Psi^{t}). \tag{41}$$

Here $\bar{k}_{z_2}'$ is given in Eq. (31) and the phase Ψ^{t} is given by

$$\Psi^{t}(\mathbf{r},t;k_y) = \sqrt{\alpha}\gamma^2(\bar{\omega}' + c\beta\bar{k}_{z_2}')t - k_y y$$
$$- \sqrt{\alpha}\gamma^2[(\bar{\omega}'\beta c^{-1} + \bar{k}_{z_2}')z + (\bar{k}_{z_1}' - \bar{k}_{z_2}')z_0]. \tag{42}$$

Note that, by evaluating $\tilde{\mathbf{D}}^{t}$ and $\tilde{\mathbf{B}}^{t}$ in the same manner, the resulting spectral PWs and the ones in Eq. (41) satisfy the constitutive relations in Eq. (8) by replacing ε_1' and μ_1' with ε_2' and μ_2', respectively.

4. ASYMPTOTIC EVALUATION IN *K*′-FRAME

In the high-frequency regime, the dominant contributions to the scattered field spectral integrals in Eqs. (19), (27), and (32) arise from the vicinity of spectral saddle points. In order to evaluate the spectral integrals asymptotically, it is convenient to apply here the spectral angle $\tilde{\varphi}$, which is defined for a given spectral wavenumber k_y by the transformation

$$k_y = \bar{k}_1 \sin \tilde{\varphi}. \tag{43}$$

The spectral angle eliminates the branch points $k_y = \pm\bar{k}_1$ of the spectral k_y integrals since $\bar{k}_{z_1} = \bar{k}_1 \cos \tilde{\varphi}$. Next we evaluate the incident and scattered fields in K'-frame asymptotically and identify the associated relativistic wave phenomena.

A. Incident Wave

To simplify the form of spectral integrals in Eq. (19), we introduce the incident wave coordinates, $(R^{i'}, \varphi^{i'})$, that are defined for a given event $(y', \bar{z}', \bar{t}')$ by the transformation [see Fig. 4(a)]

$$R^{i'} \cos \varphi^{i'} = \bar{z}' + v\bar{t}', \qquad R^{i'} \sin \varphi^{i'} = y'. \tag{44}$$

By using these coordinates and $\tilde{\varphi}$ in Eq. (43), we recast Eq. (19) in the Fourier integral form:

$$\mathbf{E}^{i'}(\mathbf{r}', t') = -\hat{\mathbf{x}} I^i(\mathbf{r}', t') \exp(j\Psi_0^{i'}), \qquad \Psi_0^{i'} = \gamma\alpha\omega t' + \beta n_1' \bar{k}_1 \bar{z}'. \tag{45}$$

In Eq. (45), $I^i(\mathbf{r}', t')$ denotes the spectral integral

$$I^i(\mathbf{r}', t') = \frac{1}{2\pi} \int_C \mathrm{d}\tilde{\varphi} f^i(\tilde{\varphi}) \exp[j\Psi^{i'}(\mathbf{r}', t'; \tilde{\varphi})] \tag{46}$$

over the integration contour in Fig. 3, where the phase $\Psi^{i'}(\tilde{\varphi})$ and the amplitude $f^i(\tilde{\varphi})$ are given by

$$\Psi^{i'}(\mathbf{r}', t'; \tilde{\varphi}) = -\bar{k}_1 R^{i'} \cos(\tilde{\varphi} - \varphi^{i'}), \qquad f^i(\tilde{\varphi}) = I_0 \mu_1' \sqrt{\alpha}\omega'/2. \tag{47}$$

Here ω' that is defined in Eq. (23) is a function of $\tilde{\varphi}$:

$$\omega'(\tilde{\varphi}) = \omega\gamma\alpha(1 - n_1'\beta \cos \tilde{\varphi}). \tag{48}$$

Upon setting $\partial_{\tilde{\varphi}}\Psi^{i'} = \bar{k}_1 R^{i'} \sin(\tilde{\varphi} - \varphi^{i'}) = 0$, we find that the phase in Eq. (47) has a saddle point $\tilde{\varphi}_s^i = \varphi^{i'}$. The amplitude $f^i(\tilde{\varphi})$ has no singularities near the saddle point and the integral in Eq. (46) can be evaluated asymptotically along the steepest descent path (SDP) using the isolated saddle point contribution [15]:

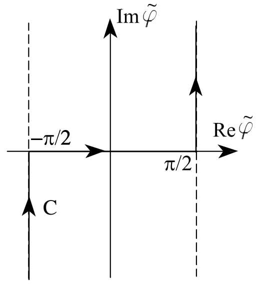

Fig. 3. Integration contour in the spectral $\tilde{\varphi}$ plane.

$$I^i(\mathbf{r}', t') \sim I^i_{\mathrm{SDP}} = \sqrt{\frac{1}{2\pi|\partial^2_{\tilde{\varphi}}\Psi^{i'}(\tilde{\varphi}_s^i)|}} f^i(\tilde{\varphi}_s^i) \times \exp[j\Psi^{i'}(\tilde{\varphi}_s^i) \pm j\pi/4], \tag{49}$$

where the $\pm$ sign corresponds to $\partial^2_{\tilde{\varphi}}\Psi^{i'}(\tilde{\varphi}_s^i) \lessgtr 0$.

By inserting Eqs. (47) into Eq. (49), we obtain

$$I^i_{\mathrm{SDP}} = \sqrt{\alpha}\mu_1'\omega'(\varphi^{i'}) \frac{I_0 \exp(-j\bar{k}_1 R^{i'} - j\pi/4)}{\sqrt{8\pi\bar{k}_1 R^{i'}}}, \tag{50}$$

where $\omega'(\varphi^{i'})$ is obtained from Eq. (48).

In a similar manner, using $\tilde{\mathbf{H}}^{i'}$ in Eq. (20) as well as $\tilde{\varphi}$ in Eq. (43) and the coordinates in Eq. (44), we obtain

$$\mathbf{H}^{i'}(\mathbf{r}', t') \sim \frac{1}{\eta_1'} I^i_{\mathrm{SDP}} \exp(j\Psi_0^{i'})\hat{\mathbf{h}}^{i'}(\varphi^{i'}),$$
$$\hat{\mathbf{h}}^{i'}(\varphi^{i'}) = \frac{-\hat{\mathbf{y}}(\cos \varphi^{i'} - n_1'\beta) + \hat{\mathbf{z}} \sin \varphi^{i'}/(\gamma\sqrt{\alpha})}{(1 - \beta n_1' \cos \varphi^{i'})}, \tag{51}$$

where $\eta_1' = \sqrt{\mu_1'/\varepsilon_1'}$.

The physical interpretation of the asymptotic field in Eq. (50) is plotted in Fig. 4(a). At time t', the normalized time $\bar{t}' = \sqrt{\alpha}\gamma t'$ so the source is located in $\bar{z}' = -v\bar{t}'$ over the $\bar{z}'$ axis. The source is moving at constant speed away from the stationary interface at $\bar{z}' = \bar{z}_0'$. Here $R^{i'}$ in Eq. (44) is identified as the distance from the moving source to the observation space–time event $(y', \bar{z}', \bar{t}')$. The asymptotic scalar field I^i_{SDP} resembles the 2D asymptotic scalar Green's function in free space in which the phase is commutated along $R^{i'}$. Thus the main contribution to the integral in Eq. (19) arises from the ray that emanates from the moving source and moves along the straight line to the observation point. Apart from $R^{i'}$ dependence on t', the electric field in Eq. (45) exhibits harmonic oscillations of $\exp(\alpha\gamma\omega t')$. Note that the field accumulates an additional z'-dependent phase term in Eq. (45) due to the z-directed medium velocity.

B. Reflected Wave

The asymptotic evaluation of the reflected wave is obtained by introducing the reflected wave polar coordinates, $(R^{r'}, \varphi^{r'})$, which are defined for a given event $(y', \bar{z}', \bar{t}')$ by the transformation [see Fig. 4(b)]

$$R^{r'} \cos \varphi^{r'} = 2\bar{z}_0' - \bar{z}' + v\bar{t}', \qquad R^{r'} \sin \varphi^{r'} = y'. \tag{52}$$

By using Eq. (52), we recast the spectral integrals in Eq. (27) in the form

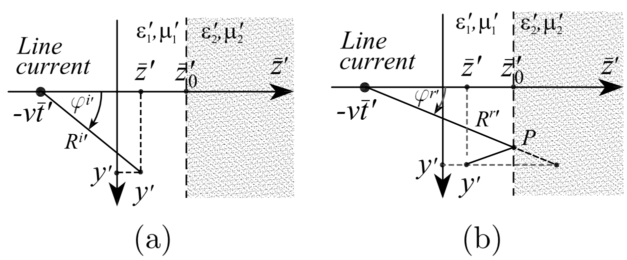

Fig. 4. Geometrical optics interpretation of the ray field forms: (a) the incident field in Eq. (50) and (b) the reflected field in Eq. (58).

$$\mathbf{E}^{r'}(\mathbf{r}',t') = -\hat{\mathbf{x}}I^r(\mathbf{r}',t')\exp(j\Psi_0^{r'}),$$
$$\Psi_0^{r'} = \gamma\alpha\omega t' - \beta n_1'\bar{k}_1(\bar{z}' - 2\bar{z}_0'). \tag{53}$$

In Eq. (53), $I^r(\mathbf{r}',t')$ denotes the spectral integral

$$I^r(\mathbf{r}',t') = \frac{1}{2\pi}\int_C \mathrm{d}\tilde{\varphi} f^r(\tilde{\varphi})\exp[j\Psi^{r'}(\mathbf{r}',t';\tilde{\varphi})], \tag{54}$$

over the integration contour in Fig. 3 with

$$\Psi^{r'}(\mathbf{r}',t';\tilde{\varphi}) = -\bar{k}_1 R^{r'}\cos(\tilde{\varphi}-\varphi^{r'}), \quad f^r(\tilde{\varphi}) = \Gamma'(\tilde{\varphi})f^i(\tilde{\varphi}), \tag{55}$$

with $f^i(\tilde{\varphi})$ in Eq. (47). $\Gamma'(\tilde{\varphi})$ denotes the reflection coefficient

$$\Gamma'(\tilde{\varphi}) = \frac{\mu_2'(\cos\tilde{\varphi} - n_1'\beta) - \mu_1'\sqrt{n_{21}'^2(1-n_1'\beta\cos\tilde{\varphi})^2 - \sin^2\tilde{\varphi}/(\alpha\gamma^2)}}{\mu_2'(\cos\tilde{\varphi} - n_1'\beta) + \mu_1'\sqrt{n_{21}'^2(1-n_1'\beta\cos\tilde{\varphi})^2 - \sin^2\tilde{\varphi}/(\alpha\gamma^2)}}, \tag{56}$$

with $n_{21}' \equiv n_2'/n_1'$. The reflection coefficient has two branch points that are denoted by $\tilde{\varphi}_{b_{1,2}}$. By setting the square root in Eq. (56) to zero, we obtain in range $|\tilde{\varphi}_{b_{1,2}}| \le \pi/2$

$$\cos\tilde{\varphi}_{b_{1,2}} = \frac{n_{21}'n_2'\beta\alpha\gamma^2 \pm \sqrt{(n_{21}'n_2'\beta\alpha\gamma^2)^2 - (n_2'^2\beta^2\alpha\gamma^2+1)(n_{21}'^2\alpha\gamma^2-1)}}{n_2'^2\beta^2\alpha\gamma^2+1}. \tag{57}$$

The branch points define two relativistic critical angles for which the spectral transferred PWs propagate parallel to the interface [see Eq. (36)].

The integral in Eq. (54) has the stationary point $\tilde{\varphi}_s^r = \varphi^{r'}$. We distinguish two scattering regimes: under critical angle incidence in which $\tilde{\varphi}_{b_1} < \tilde{\varphi}_s^r < \tilde{\varphi}_{b_2}$ and over critical angle incidence in which either $\tilde{\varphi}_s^r < \tilde{\varphi}_{b_1}$ or $\tilde{\varphi}_s^r > \tilde{\varphi}_{b_2}$.

1. Under Critical Angle Incidence

The integration contour in this regime can be deformed into integral along the SDP as plotted in Fig. 5(a). The reflected wave is evaluated asymptotically by using the isolated saddle point contribution in (49). This procedure yields

$$I^r \sim I_{\mathrm{SDP}}^r = \Gamma'(\varphi^{r'})\sqrt{\alpha}\mu_1'\omega'(\varphi^{r'})\frac{I_0\exp(-j\bar{k}_1R^{r'} - j\pi/4)}{\sqrt{8\pi\bar{k}_1R^{r'}}}, \tag{58}$$

where, from Eq. (48), $\omega'(\varphi^{r'}) = \omega\gamma\alpha(1-\beta n_1'\cos\varphi^{r'})$. In a similar manner, by using $\tilde{H}^{r'}$ in Eq. (28) we obtain

$$\mathbf{H}^{r'}(\mathbf{r}',t') \sim \frac{1}{\eta_1'}I_{\mathrm{SDP}}^r\exp(j\Psi_0^{r'})\hat{\mathbf{h}}^{r'}(\varphi^{r'}),$$
$$\hat{\mathbf{h}}^{r'}(\varphi^{r'}) = \frac{\hat{\mathbf{y}}(\cos\varphi^{r'} - n_1'\beta) + \hat{\mathbf{z}}\sin\varphi^{r'}/(\gamma\sqrt{\alpha})}{(1-\beta n_1'\cos\varphi^{r'})}. \tag{59}$$

The physical interpretation of the asymptotic EM field in Eq. (58) is plotted in Fig. 4(b). The source, which is located in $\bar{z}' = -v\bar{t}'$ over the $\bar{z}'$ axis, is moving at speed v away from the stationary interface. Here $R^{r'}$ in Eq. (52) is identified as the length of the reflected ray from the interface to the observation space–time event $(y',\bar{z}',\bar{t}')$. The ray path satisfies Snell's law in $(y',\bar{z}')$ space (i.e., the angle of reflection equals the angle of incidence at time $\bar{t}'$).

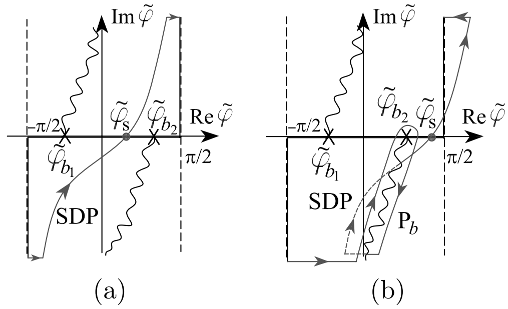

Fig. 5. Integration contour in $\tilde{\varphi}$ plane for the reflected field (a) under and (b) over critical angle incidence.

2. Over Critical Angle Incidence

The reflected field asymptotic evaluation for over critical angle incidence is preformed by deforming the integration path of I^r in Eq. (54) to the integration contour in Fig. 5(b). The electric field is consist of two contributions

$$\mathbf{E}^{r'}(\mathbf{r}',t') = \mathbf{E}_{\mathrm{SDP}}^{r'}(\mathbf{r}',t') + \mathbf{E}_b^{r'}(\mathbf{r}',t'), \tag{60}$$

where $\mathbf{E}_{\mathrm{SDP}}^{r'}$ denotes the contribution of the integration along the SDP and $\mathbf{E}_b'$ denotes the contribution of the integration around the branch cut of $\tilde{\varphi}_{b_1}$ (or $\tilde{\varphi}_{b_2}$) in Eq. (57). The asymptotic SDP contribution that arises from the vicinity of the stationary point in the upper Riemann sheet is given in Eq. (53) with Eq. (58).

In the high-frequency regime, the main contribution to $\mathbf{E}_b'$ arises from points in the vicinity of the corresponding branch point in the upper Riemann sheet [16]. Therefore, in order to evaluate $\mathbf{E}_b'$ asymptotically, we apply a first-order Taylor approximation to $\Gamma'(\tilde{\varphi})$ in Eq. (56) about the branch point. Thus, for $\tilde{\varphi} \approx \tilde{\varphi}_{b_{1,2}}$,

$$\Gamma'(\tilde{\varphi}) \simeq 1 + j2\mu_1'\frac{\sqrt{2\sin\tilde{\varphi}_{b_{1,2}}}\sqrt{\tilde{\varphi} - \tilde{\varphi}_{b_{1,2}}}}{\gamma\sqrt{\alpha}\sqrt{(\cos\tilde{\varphi}_{b_{1,2}} - n_1'\beta)(1-n_1'\beta\cos\tilde{\varphi}_{b_{1,2}})}}. \tag{61}$$

Equation (54) with Eq. (61) has the generic form of the branch-cut integral [16]:

$$I_b = \int_{P_b}\mathrm{d}\tilde{\varphi}\left(a + b\sqrt{\tilde{\varphi} - \tilde{\varphi}_b}\right)\exp[\Omega q(\tilde{\varphi})]$$
$$\sim \frac{b\sqrt{\pi}}{[-\Omega q'(\tilde{\varphi}_b)]^{3/2}}\exp[\Omega q(\tilde{\varphi}_b)], \tag{62}$$

where P_b is a contour encircling the branch cut in the positive sense [see Fig. 5(b)], Ω is a large parameter, a and b are constants, $q(\tilde{\varphi})$ is a regular in the vicinity of $\tilde{\varphi}_b$, and $\exp[\Omega q(\tilde{\varphi})]$ decays along the contour. Thus, by applying Eq. (62) to Eq. (54) with Eqs. (57) and (61) for large real k_1 values we obtain

$$\mathbf{E}_b^{r'}(\mathbf{r}',t') \sim -\hat{\mathbf{x}} E_{b1}^{r'} D' E_{b2}^{r'} E_{b3}^{r'} \exp(j\alpha\gamma\omega t'), \tag{63}$$

where

$$E_{b1}^{r'} = \frac{I_0\sqrt{\alpha}\mu_1'\omega'(\varphi^r)}{\sqrt{8\pi\bar{k}_1 L_1'}} \exp(j\Psi_{b1}'), \tag{64}$$

with

$$\Psi'_{b1} = -\bar{k}_1 L_1' - (\pi/4) + \beta n_1'\bar{k}_1\bar{z}_0', \qquad L_1' = (\bar{z}_0' - v\bar{t}')/\cos\theta_c'. \tag{65}$$

By comparing Eq. (64) to Eqs. (45) with (50), E_{b1}' is identified as the incident ray that propagates from the source and impinges on the interface at the critical angle (angle of total reflection) θ_c' that is defined by

$$\sin\theta_c' = n_{21}' \tag{66}$$

(see Fig. 6). The D' term in Eq. (63), which is given by

$$D' = \frac{2j\sin^2\theta_c'\sqrt{\bar{k}_1 L_1'}}{\sqrt{\alpha}\gamma(\cos\theta_c')^{3/2}\sqrt{\cos\theta_c' - n_1'\beta}\sqrt{1 - n_1'\beta\cos\theta_c'}}, \tag{67}$$

is identified as the relativistic *diffraction coefficient*. The $E_{b2}^{r'}$ and $E_{b3}^{r'}$ terms in Eq. (63) are given by

$$E_{b2}^{r'} = \frac{\exp(-j\bar{k}_2 L_2')}{(\bar{k}_2 L_2')^{3/2}}, \qquad L_2' = y' - L_1'\sin\theta_c' + (\bar{z}' - \bar{z}_0')\tan\theta_c', \tag{68}$$

where $\bar{k}_2 = \omega\sqrt{\alpha\epsilon_2'\mu_2'}$, and

$$E_{b3}^{r'} = \exp(-j\bar{k}_1 L_3')\exp[j\beta n_1'\bar{k}_1(\bar{z}_0' - \bar{z}')],$$
$$L_3' = (\bar{z}_0' - \bar{z}')/\cos\theta_c'. \tag{69}$$

The $E_{b2}^{r'}$ field term in Eq. (68) describes the relativistic lateral ray that is propagating along L_2' parallel to the interface in the $z' = z_0'^{+}$ medium. The lateral ray $(\bar{k}_2 L_2')^{-3/2}$ decay along its trajectory is due to the $E_{b3}^{r'}$ field radiation back to n_1' medium. By comparing Eqs. (53) with (58) to Eq. (69), the $E_{b3}^{r'}$ field term is identified as the ray that is propagating from the interface at angle θ_c' to the observation point (y', z') along L_3' (see Fig. 6).

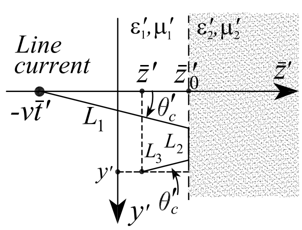

Fig. 6. Geometrical optics interpretation of the lateral (head) wave in Eq. (63).

Finally, by sampling the amplitude of $\tilde{\mathbf{H}}^{r'}$ in Eq. (28) at $\tilde{\varphi} = \tilde{\varphi}_{b_{1,2}}$ and applying the same analytic procedure, we obtain the asymptotic head-wave magnetic field:

$$\mathbf{H}_b^{r'}(\mathbf{r}',t') \sim \frac{1}{\eta_1'} E_{b1}^{r'} D' E_{b2}^{r'} E_{b3}^{r'} \exp(j\alpha\gamma\omega t')\hat{\mathbf{h}}^{r'}(\tilde{\varphi}_{b_{1,2}}),$$
$$\hat{\mathbf{h}}^{r'}(\tilde{\varphi}_{b_{1,2}}) = \frac{\hat{\mathbf{y}}(\cos\tilde{\varphi}_{b_{1,2}} - n_1'\beta) + \hat{\mathbf{z}}\sin\tilde{\varphi}_{b_{1,2}}/(\gamma\sqrt{\alpha})}{(1 - \beta n_1'\cos\tilde{\varphi}_{b_{1,2}})}. \tag{70}$$

C. Transmitted Field

The exact transmitted EM field in K'-frame is given by a spectral representation in Eq. (32). To simplify the form of the spectral integrals, we introduce the transmitted wave polar coordinates, $(R_1^{t'}, R_2^{t'}, \varphi_1^{t'}, \varphi_2^{t'})$, that are defined for a given space–time event (y', z', t') by the transformation (see Fig. 7)

$$R_1^{t'}\cos\varphi_1^{t'} = \bar{z}_0' + v\bar{t}', \quad R_2^{t'}\cos\varphi_2^{t'} = \bar{z}' - \bar{z}_0', \tag{71}$$

where angles $\varphi_1^{t'}$ and $\varphi_2^{t'}$ satisfy

$$\tan\varphi_2^{t'} = \frac{(n_{21}'\alpha\gamma^2)^{-1}\sin\varphi_1^{t'} - n_2'(1 - n_1'\beta\cos\varphi_1^{t'})\beta\tan\varphi_1^{t'}}{\sqrt{(1 - n_1'\beta\cos\varphi_1^{t'})^2 - \sin^2\varphi_1^{t'}/n_{21}'^2\alpha\gamma^2}}. \tag{72}$$

Equation (72) is identified later as the relativistic Snell's law [see discussion following Eq. (83)]. Note that, by inverting the transformation in Eq. (71), we obtain

$$y' = R_1^{t'}\sin\varphi_1^{t'} + R_2^{t'}\sin\varphi_2^{t'}. \tag{73}$$

By using Eq. (71) and the complex angle $\tilde{\varphi}$ in Eq. (43), we recast the spectral integrals in Eq. (32) in the form

$$\mathbf{E}^{t'}(\mathbf{r}',t') = -\hat{\mathbf{x}}\exp[j\Psi_0^{i'}(\mathbf{r}',t')]I^t(\mathbf{r}',t'),$$
$$I^t(\mathbf{r}',t') = \frac{1}{2\pi}\int_C \mathrm{d}\tilde{\varphi} f^t(\tilde{\varphi})\exp[j\Psi^{t'}(\mathbf{r}',t';\tilde{\varphi})], \tag{74}$$

where $\Psi_0^{i'}$ is given in Eq. (45), the amplitude

$$f^t(\tilde{\varphi}) = T'(\tilde{\varphi})f^i(\tilde{\varphi}), \tag{75}$$

with f^i in Eq. (47), and the spectral phase $\Psi^{t'}(\tilde{\varphi})$ is given by

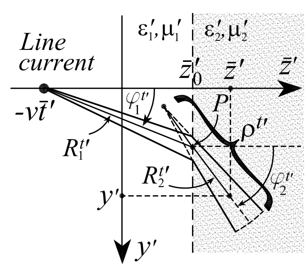

Fig. 7. Geometrical optics interpretation of asymptotic transferred field in Eq. (80).

$$\Psi^{t\prime}(\mathbf{r}', t'; \tilde{\varphi}) = -\bar{k}_1\left[R_1^{t\prime}\cos(\tilde{\varphi} - \varphi_1^{t\prime}) + R_2^{t\prime}\left(\sin\,\varphi_2^{t\prime}\,\sin\,\tilde{\varphi} + n'_{21}\,\cos\,\varphi_2^{t\prime}\sqrt{(1 - n'_1\beta\,\cos\,\tilde{\varphi})^2 - \sin^2\tilde{\varphi}/n'^2_{21}\alpha\gamma^2}\right)\right]. \quad (76)$$

The Fresnel transmission coefficient in the amplitude in Eq. (75) in terms of the spectral angle $\tilde{\varphi}$ is given by

$$T'(\tilde{\varphi}) = \frac{2\mu'_2(\cos\,\tilde{\varphi} - n'_1\beta)}{\mu'_2(\cos\,\tilde{\varphi} - n'_1\beta) + \mu'_1 n'_{21}\sqrt{(1 - n'_1\beta\,\cos\,\tilde{\varphi})^2 - \sin^2\tilde{\varphi}/n'^2_{21}\alpha\gamma^2}}. \quad (77)$$

The stationary point that is denoted by $\tilde{\varphi}_{s1}$ is obtained by setting $\partial_{\tilde{\varphi}}\Psi^{t\prime}(\tilde{\varphi})|_{\tilde{\varphi}_{s1}} = 0$. By using Eqs. (71), (75), and (76), we find that $\tilde{\varphi}_{s1}$ satisfies

$$y' - \tan\,\tilde{\varphi}_{s1}(\bar{z}'_0 + vt') - \tan\,\tilde{\varphi}_{s2}(\bar{z}' - \bar{z}'_0) = 0, \quad (78)$$

where $\tilde{\varphi}_{s2}$ is related to $\tilde{\varphi}_{s1}$ by

$$\tan\,\tilde{\varphi}_{s2} = \frac{(n'_{21}\alpha\gamma^2)^{-1}\,\sin\,\tilde{\varphi}_{s1} - n'_2(1 - n'_1\beta\,\cos\,\tilde{\varphi}_{s1})\beta\,\tan\,\tilde{\varphi}_{s1}}{\sqrt{(1 - n'_1\beta\,\cos\,\tilde{\varphi}_{s1})^2 - \sin^2\tilde{\varphi}_{s1}/n'^2_{21}\alpha\gamma^2}}. \quad (79)$$

By comparing Eqs. (78) and (79) with Eqs. (72) and (73), we deduce that $\tilde{\varphi}_{s1} = \varphi_1^{t\prime}$ and, therefore, $\tilde{\varphi}_{s2} = \varphi_2^{t\prime}$.

By inserting Eqs. (78), (79) with (77) and (76), (75) into (49), we obtain the asymptotic expression of the transferred field:

$$\mathbf{E}^{t\prime}(\mathbf{r}', t') \sim -\hat{\mathbf{x}}E_1^{t\prime}E_2^{t\prime}\,\exp(j\omega\gamma\alpha t'), \quad (80)$$

where

$$E_1^{t\prime} = \sqrt{\alpha}\mu'_1\omega'(\varphi_1^{t\prime})\frac{I_0\,\exp(-j\bar{k}_1 R_1^{t\prime} + j\beta n'_1\bar{k}_1\bar{z}'_0 - j\pi/4)}{\sqrt{8\pi\bar{k}_1 R_1^{t\prime}}} \quad (81)$$

and

$$E_2^{t\prime} = \frac{T'(\varphi_1^{t\prime})\,\exp(-j\bar{k}_2 R_2^{t\prime})}{\sqrt{1 + R_2^{t\prime}/\rho^{t\prime}}}, \quad (82)$$

where $T'(\varphi_1^{t\prime})$ is given in Eq. (77), and

$$\rho^{t\prime} = \frac{R_1^{t\prime}}{\sin\,\varphi_2^{t\prime}\cos^2\varphi_1^{t\prime}} \times\left[\frac{n'_{12}[1 - \beta^2(n'^2_1 - n'^2_2)]\sin\,\varphi_1^{t\prime} - n'_2\beta\,\tan\,\varphi_1^{t\prime}}{n'_{12}[1 - \beta^2({n'_1}^2 - {n'_2}^2)] - n'_2\beta/\cos^3\varphi_1^{t\prime} + n'_{12}\tan^2\varphi_2^{t\prime}}\right]. \quad (83)$$

Equation (78) sets the ray path that is shown in Fig. 7, where observation event $(y', \bar{z}', t')$ is represented by $\varphi_1^{t\prime}$, $\varphi_2^{t\prime}, R_1^{t\prime}, R_2^{t\prime}$ via Eq. (71). Following this definition, we identify Eq. (78) as the path from the source along a straight line with angles $\tilde{\varphi}^t_{s1,2} = \varphi^{t\prime}_{1,2}$ and lengths $R^{t\prime}_{1,2}$ in $\bar{z}' < \bar{z}'_0$ or $\bar{z}' > \bar{z}'_0$, respectively. Thus Eq. (79) [or Eq. (72)] describes the relativistic Snell's law for this specific scattering scenario. This relation adjusts the angles to the source velocity. The spectral Doppler shift in Eq. (23) changes the conventional (stationary) Snell's law, which is obtained for (K'-frame) time-harmonic excitation. Note that, by setting $\beta = 0$ in Eq. (79), we obtained the well-known (stationary) Snell's law.

The transferred field in Eq. (80) consists of $E_1^{t\prime}$ in Eq. (81) and $E_2^{t\prime}$ in Eq. (82). By using Eq. (50) in Eq. (45), $E_1^{t\prime}$ is identified as the incident electric field at point P over the interface. This point is the intersection of the incident ray, which is emanating from the source with departure angle $\varphi_1^{t\prime}$ and the interface at $\bar{z}' = \bar{z}_0{}'$. Thus, $R_1^{t\prime}$ is identified as the radius of curvature of the incident wavefront at point P (see Fig. 7). The second term in the transferred field, $E_2^{t\prime}$, is identified as the ray field that is propagating in $\bar{z}' > \bar{z}_0{}'$ medium along the optical path $R_1^{t\prime}$. By using Eq. (83), we identify $\rho^{t\prime}$ as the principal radius of curvature of the transferred wavefront at point P.

The corresponding magnetic transferred field is obtained from Eq. (33), giving

$$\mathbf{H}^{t\prime}(\mathbf{r}', t') \sim \frac{1}{\eta'_2}E_1^{t\prime}E_2^{t\prime}\,\exp(j\omega\gamma\alpha t')\hat{\mathbf{h}}^{t\prime}(\varphi^{i\prime}),$$
$$\hat{\mathbf{h}}^{t\prime}(\varphi^{i\prime}) = \frac{-\hat{\mathbf{y}}\,\cos\,\varphi_2^{t\prime} + \hat{\mathbf{z}}\,\sin\,\varphi_1^{t\prime}/\left(n'_{21}\gamma\sqrt{\alpha}\right)}{(1 - n'_1\beta\,\cos\,\varphi_1^{t\prime})}. \quad (84)$$

5. ASYMPTOTIC FIELDS IN *K*-FRAME

A. Incident Field

The asymptotic fields in K'-frame are transformed to K-frame by applying the inverse field transformation of Eq. (4) and ILT Eq. (2) to Eqs. (45), (50), and (51) with K'-frame constitutive relations in Eq. (7). This results in

$$\mathbf{E}^i(\mathbf{r}, t) \sim -\hat{\mathbf{x}}E_x^i(\mathbf{r})\,\exp(j\omega t),$$
$$E_x^i(\mathbf{r}) = I_0\omega\mu'_1\alpha^{1/2}\frac{\exp[-j\bar{k}_1 R^i - j\pi/4]}{\sqrt{8\pi\bar{k}_1 R^i}}\,\exp(jkmz),$$
$$\mathbf{H}^i(\mathbf{r}, t) \sim \frac{1}{\eta'_1}E_x^i(\mathbf{r})\,\exp(j\omega t)\left(-\hat{\mathbf{y}}\,\cos\,\varphi^i + \hat{\mathbf{z}}\,\sqrt{\alpha}\sin\,\varphi^i\right), \quad (85)$$

where $R^i = \sqrt{y^2 + \bar{z}^2}$ and $\cos\,\varphi^i = \bar{z}/R^i$. These expressions are used later for identifying the incident ray field contribution to the reflected and transmitted fields.

B. Reflected Field

In Subsection 4.B we distinguished two reflection regimes in which the K'-frame incident ray is impinging on the interface with an angle that is larger or smaller than the critical angle. In this subsection, we identify the K-frame relativistic wave phenomena associated with these two scattering regimes.

1. Under Critical Angle Incidence

The under critical angle scattering regime for which in K'-frame $\tilde{\varphi}_{b_1} < \tilde{\varphi}_s^r < \tilde{\varphi}_{b_2}$ was investigated in Subsection 4.B.1. By applying ILT we obtained that, in K-frame, the stationary point is given by

$$\tilde{\varphi}_s^r = \cos -1\left[\frac{\gamma^2\sqrt{\alpha}[2(z_0+vt)-z(1+\beta^2)]}{\sqrt{y^2+\gamma^4\alpha[2(z_0+vt)-z(1+\beta^2)]^2}}\right]. \tag{86}$$

By inserting Eqs. (53) and (59) with Eq. (58) into Eq. (7) and then into the field transformation in Eq. (4) and using ILT in Eq. (2), we obtain the reflected field (isolated saddle point contribution) in K-frame in the form

$$\mathbf{E}^r(\mathbf{r},t) \sim -\hat{\mathbf{x}}E_x^r(\mathbf{r},t)\exp(j\Psi^r), \tag{87}$$

where

$$\Psi^r = \gamma^2\alpha(1+\beta^2 n_1'^2)\omega t - \beta\gamma^2\sqrt{\alpha}\bar{k}_1[z(1+n_1'^2)/n_1' - 2n_1' z_0],$$
$$E_x^r(\mathbf{r},t) = \omega\mu_1'\gamma^2\alpha^{3/2}\Gamma(\varphi^r)\frac{I_0\exp\left(-j\bar{k}_1R^r - j\frac{\pi}{4}\right)}{\sqrt{8\pi\bar{k}_1R^r}}, \tag{88}$$

with

$$R^r = \sqrt{y^2+\gamma^4\alpha[2(z_0+vt)-z(1+\beta^2)]^2},$$
$$\cos\varphi^r = \gamma^2\sqrt{\alpha}[2(z_0+vt)-z(1+\beta^2)]/R^r,$$
$$\Gamma(\varphi^r) = (1-2\beta n_1'\cos\varphi^r+\beta^2 n_1'^2)\Gamma'(\varphi^r). \tag{89}$$

Γ' is given in Eq. (56).

In a similar manner,

$$\mathbf{H}^r(\mathbf{r},t) \sim \frac{1}{\eta_1'}E_x^r\exp(j\Psi^r)\hat{\mathbf{h}}^r(\varphi^r),$$
$$\hat{\mathbf{h}}^r(\varphi^r) = \frac{\hat{\mathbf{y}}[\cos\varphi^r(1+\beta^2n_1'^2)-2\beta n_1'] + \hat{\mathbf{z}}\sin\varphi^r/\gamma^2\sqrt{\alpha}}{1-2\beta n_1'\cos\varphi^r+\beta^2n_1'^2}. \tag{90}$$

2. Over Critical Angle Incidence

The over critical angle scattering regime for which, in K'-frame, $\tilde{\varphi}_s^r < \tilde{\varphi}_{b_1}$ or $\tilde{\varphi}_s^r > \tilde{\varphi}_{b_1}$ was investigated in Subsection 4.B.2. $\tilde{\varphi}_s^r$ in K-frame is given in Eq. (86). Following the discussion preceding Eq. (60), the reflected electric field consists of two contributions

$$\mathbf{E}^r(\mathbf{r},t) = \mathbf{E}^r_{\mathrm{SDP}}(\mathbf{r},t) + \mathbf{E}^r_b(\mathbf{r},t), \tag{91}$$

where $\mathbf{E}^r_{\mathrm{SDP}}$ denotes the contribution of the integration along the SDP, which is given in Eq. (87), and $\mathbf{E}_b$ denotes the contribution of the integration around the branch cut of $\tilde{\varphi}_{b_1}$ (or $\tilde{\varphi}_{b_2}$) in Eq. (57). Following the K'-frame representation in Eq. (63), we define

$$L_1 = \sqrt{\alpha}\gamma^2(z_0+\beta^2z-vt)/\cos\theta_c',$$
$$L_3 = \sqrt{\alpha}\gamma^2(z_0-z+vt)/\cos\theta_c',$$
$$L_2 = R^r\sin\varphi^r - L_1\sin\theta_c' + \sqrt{\alpha}\gamma^2(z-z_0-vt)\tan\theta_c'. \tag{92}$$

By inserting Eqs. (63) and (70) into Eq. (7) and then into the field transformation in Eq. (4) and using ILT in Eq. (2), we obtain

$$\mathbf{E}_b^r(\mathbf{r},t) \sim -\hat{\mathbf{x}}E_{b1}^rDE_{b2}^rE_{b3}^r\exp[j\alpha\gamma^2\omega(t-\beta z/c)], \tag{93}$$

where

$$E_{b1}^r = \frac{I_0\gamma^2\alpha^{3/2}\mu_1'\omega(\varphi^r)}{\sqrt{8\pi\bar{k}_1L_1}}(1-2\beta n_1'\cos\varphi^r+\beta^2n_1'^2)\exp(j\Psi_{b1}), \tag{94}$$

with

$$\Psi_{b1} = -\bar{k}_1L_1 - \pi/4 + \beta n_1'\bar{k}_1\sqrt{\alpha}\gamma^2 z_0. \tag{95}$$

By comparing Eq. (64) to Eqs. (45) with (50), E_{b1}^r is identified as the incident ray that propagates from the source and impinges on the interface at the critical angle θ_c' in Eq. (66). The D term in Eq. (93), which is given by

$$D = \frac{2j\sin\theta_c'\sqrt{\bar{k}_1L_1}}{\sqrt{\alpha}\gamma(\cos\theta_c')^{3/2}\sqrt{\cos\theta_c' - n_1'\beta}\sqrt{1-n_1'\beta\cos\theta_c'}}, \tag{96}$$

is identified as the relativistic *diffraction coefficient*. The E_{b2}^r and E_{b3}^r terms in Eq. (93) are given by

$$E_{b2}^r = \frac{\exp(-j\bar{k}_2L_2)}{(\bar{k}_2L_2)^{3/2}}, \tag{97}$$

$$E_{b3}^r = \exp(-j\bar{k}_1L_3)\exp[j\beta n_1'\bar{k}_1\sqrt{\alpha}\gamma^2(z_0-z+vt)]. \tag{98}$$

C. Transferred Field

By applying the field transformation to Eq. (80), we obtain the asymptotic refracted fields in K-frame:

$$\mathbf{E}_x^t(\mathbf{r},t) \sim -\hat{\mathbf{x}}E_1^t(\mathbf{r},t)E_2^t(\mathbf{r},t)\exp[j\alpha\gamma^2\omega(t-\beta z/c)], \tag{99}$$

where

$$E_1^t = I_0\mu_1'\gamma^2\alpha^{3/2}\omega(\varphi_1^t)\frac{\exp(-j\bar{k}_1R_1^t + j\bar{k}_1n_1'\beta\sqrt{\alpha}\gamma^2z_0 - j\pi/4)}{\sqrt{8\pi\bar{k}_1R_1^t}},$$
$$E_2^t = \frac{T(\varphi_1^t)\exp(-j\bar{k}_2R_2^t)}{\sqrt{1+R_2^t/\rho^t}}, \tag{100}$$

with $T(\varphi_1^t) = T'(1-n_1'\beta\cos\varphi_1^t + n_2'\beta\cos\varphi_2^t)$. T' is given in Eq. (77), and

$$\cos\varphi_1^t = \sqrt{\alpha}\gamma^2(z_0+vt-\beta^2z)/R_1^t,$$
$$\cos\varphi_2^t = \sqrt{\alpha}\gamma^2(z-z_0-vt)/R_2^t, \tag{101}$$

$$R_1^t = \sqrt{y_P^2 + \alpha\gamma^4(z_0 + vt - \beta^2 z)^2},$$
$$R_2^t = \sqrt{(y - y_P)^2 + \alpha\gamma^4(z - z_0 - vt)^2}, \qquad (102)$$

where $y_P = R_1^{i\prime} \sin \varphi_1^{i\prime}$ denotes the y-axis value of the intersection point P of the incident ray and the interface (see Fig. 7).

6. CONCLUSIONS

In this paper we have investigated the canonical problem of the 2D longitudinal Green's function of a uniformly moving (lossless and dispersion-free) dielectric–magnetic medium with a planar discontinuity. The exact solution in the form of PW spectral integrals, as well as asymptotic solutions, were obtained in both the laboratory frame and the comoving frame. Interpretation of the relativistic asymptotic solutions in the form of ray fields was given. New canonical ray forms were derived for the relativistic incident fields, reflected fields, lateral wave, and transmitted (refracted) fields. This research and future investigations can eventually lead to establishing a relativistic geometrical theory of diffraction.

REFERENCES

1. C. Tai, "The dyadic Green's function for a moving isotropic medium," IEEE Trans. Antennas Propag. **13**, 322–323 (1965).
2. J. V. Bladel, *Relativity and Engineering* (Springer, 1984).
3. T. Mackay and A. Lakhtakia, "Negative phase velocity in a uniformly moving, homogeneous, isotropic, dielectric-magnetic medium," J. Phys. A **37**, 5697–5711 (2004).
4. T. Mackay, A. Lakhtakia, and S. Setiawan, "Positive-, negative-, and orthogonal-phase-velocity propagation of electromagnetic plane waves in a simply moving medium," Optik **118**, 195–202 (2007).
5. A. Lakhtakia and W. Weiglhofer, "On electromagnetic fields in a linear medium with gyrotropic-like magnetoelectric properties," Microwave Opt. Technol. Lett. **15**, 168–170 (1997).
6. A. Lakhtakia and T. Mackay, "Simple derivation of dyadic Green functions of a simply moving, isotropic, dielectric-magnetic medium," Microwave Opt. Technol. Lett. **48**, 1073–1074 (2006).
7. M. Idemen and A. Alkumru, "Relativistic scattering of a plane-wave by a uniformly moving half-plane," IEEE Trans. Antennas Propag. **54**, 3429–3440 (2006).
8. P. De Cupis, G. Gerosa, and G. Schettini, "Gaussian beam diffraction by uniformly moving targets," Atti della Fondazione Giorgio Ronchi **56**, 799–811 (2001).
9. P. D. Cupis, "Radiation by a moving wire-antenna in the presence of plane interface," J. Electromagn. Waves Appl. **14**, 1119–1132 (2000).
10. W. Arrighetti, P. De Cupis, and G. Gerosa, "Electromagnetic radiation from moving fractal sources: A plane-wave spectral approach," Prog. Electromagn. Res. **58**, 1–19 (2006).
11. P. D. Cupis, "Electromagnetic wave scattering from moving surfaces with high-amplitude corrugated pattern," J. Opt. Soc. Am. A **23**, 2538–2550 (2006).
12. T. Danov and T. Melamed, "Spectral analysis of relativistic dyadic Green's function of a moving dielectric-magnetic medium," IEEE Trans. Antennas Propag. **59**, 2973–2979 (2011).
13. J. Kong, *Theory of Electromagnetic Waves* (Wiley, 1975).
14. M. Idemen and A. Alkumru, "Influence of motion on the edge-diffraction," Prog. Electromagn. Res. B **6**, 153–168 (2008).
15. L. Felsen and N. Marcuvitz, *Radiation and Scattering of Waves* (IEEE, 1994), Chap. 4.2.
16. L. Felsen and N. Marcuvitz, *Radiation and Scattering of Waves* (IEEE, 1994), Chap. 4.8.